Optimal Sizing and Scheduling of Community Battery Storage within a Local Market

Nam Trong Dinh
trongnam.dinh@adelaide.edu.au
The University of Adelaide
Adelaide, South Australia, Australia

S. Ali Pourmousavi
a.pourm@adelaide.edu.au
The University of Adelaide
Adelaide, South Australia, Australia

Sahand Karimi-Arpanahi
sahand.karimi-arpanahi@adelaide.edu.au
The University of Adelaide
Adelaide, South Australia, Australia

Yogesh Pipada Sunil Kumar
yogeshpipada.sunilkumar@adelaide.edu.au
The University of Adelaide
Adelaide, South Australia, Australia

Mingyu Guo
mingyu.guo@adelaide.edu.au
The University of Adelaide
Adelaide, South Australia, Australia

Derek Abbott
derek.abbott@adelaide.edu.au
The University of Adelaide
Adelaide, South Australia, Australia

Jon A. R. Liisberg
jon.liisberg@watts.dk
Watts A/S
Hovedgaden, Svinninge, Denmark

ABSTRACT

The ever-increasing uptake of distributed energy resources necessitates the introduction of local electricity markets at the residential level. Electric retailers, who are adversely affected by these changes, can make a profit by operating local trading platforms and offering services through community-level battery storage. In this work, we propose a Stackelberg game-based approach for sizing the centralized battery unit under the operation of a multi-interval local market. The optimization is formulated as a bilevel program, where the leader is the market aggregator responsible for determining the local prices and battery charging/discharging schedules. Also, the followers in the bilevel program are prosumers, who can vary electricity consumption with respect to their comfort and cost of electricity. Upon obtaining the optimal capacity of the community storage, we modify the algorithm to efficiently operate the battery on a daily basis. The applicability of the proposed model is evaluated using real-world data of residential prosumers with rooftop photovoltaic systems for two different pricing schemes, which represents the profit trade-off between the aggregator and prosumers. The results show the profitability of the proposed model for community storage installation, where a relatively short payback period can be achieved via either pricing scheme.

CCS CONCEPTS

• **Hardware → Batteries**; • **Computing methodologies → Planning and scheduling**.

KEYWORDS

Community storage, local electricity market, demand response, energy rebound effect, Stackelberg game, storage sizing

ACM Reference Format:

Nam Trong Dinh, S. Ali Pourmousavi, Sahand Karimi-Arpanahi, Yogesh Pipada Sunil Kumar, Mingyu Guo, Derek Abbott, and Jon A. R. Liisberg. 2022. Optimal Sizing and Scheduling of Community Battery Storage within a Local Market. In *The Thirteenth ACM International Conference on Future Energy Systems (e-Energy '22), June 28–July 1, 2022, Virtual Event, USA*. ACM, New York, NY, USA, 13 pages. https://doi.org/10.1145/3538637.3538837

1 INTRODUCTION

The electricity grid has been transitioning to a green and sustainable system over the past couple of decades by adopting larger amount of distributed energy resources (DER) such as rooftop solar photovoltaic (PV) systems and behind-the-meter battery storage. Traditional customers can leverage their DER to lower the electricity consumption cost as well as to reduce their carbon footprint. Also, during the periods of excess solar generation, customers can export their surplus electricity to the utility grid through fixed feed-in tariff (FiT) schemes, which helps to decrease the overall energy cost. As a result, rooftop PV systems in Australia have seen a steady growth in the last decade and are expected to increase even more within the next 20 years [2].

However, the roll out of DER reduces the revenue of utility companies because of the self-consumption of PV owners in the residential sector. In other words, retailers' sale, hence their revenue, have reduced compared to the past. At the same time, the distribution network service providers are dealing with the technical and operational challenges to handle reverse power flow, which mostly occurs during mid-day. For instance, on October 31, 2021, the distribution network in South Australia (SA) observed a negative net demand for nearly four hours with a dipping record of -69.4 MW due to the high export of rooftop solar PV systems [34]. To manage it, SA Power Networks has reduced the export limit from 5 kW to 1.5 kW in some congested areas resulting in higher

e-Energy '22, June 28–July 1, 2022, Virtual Event, USA

ACM ISBN 978-1-4503-9397-3/22/06…$15.00
https://doi.org/10.1145/3538637.3538837

curtailment of renewable generation for solar customers [35]. With the increasing trend of DER, we can expect similar incidents to occur more frequently than before. Therefore, it is of great importance for electricity retailers and network operators to tackle these techno-economic challenges. While retailers can develop new business models for the consumers to avoid excessive curtailment and low FiTs, the network operators can support new energy trading platforms to facilitate the deployment of a large number of DER.

Among many possible solutions, such as time-of-use (ToU) incentives [48] or real-time prices [20], a local market that facilitates energy transactions within a community of consumers is the preferred mechanism from the perspective of customers [38]. Through a local energy trading platform, the excess energy of prosumers can be consumed by other prosumers within the local market; thus, decreasing the negative impact on the grid (e.g., lower reverse power flow) and avoiding the PV generation curtailment beyond exporting limit for prosumers [27]. In this respect, retailers can offer a trading platform to the local communities or directly participate in the market as an aggregator. This aggregator acts as an intermediary entity to facilitate the trading process for the prosumers and consumers by setting the local prices with maximization of the stakeholders' utility [26]. Within the local market region, the aggregator is responsible for exchanging surplus generation or compensating for the energy shortage with the grid. In order to add new revenue streams, community-level battery storage can be adopted to assist the energy sharing process by filling the gaps in energy production and demand [25]. Such storage units allow the aggregator to perform energy arbitrage under the ToU pricing structure, which indirectly helps network operators by decreasing reverse power flow and high load demand during peak periods [42]. The aggregator, as an entity with financial interests, is responsible for purchasing, maintaining, and operating the centralized battery unit.

In this paper, we focus on the optimal size and scheduling of the community storage to maximize the total revenue of the aggregator. The sizing problem is also integrated with demand response (load shifting) at the users' end to increase utility for all stakeholders. The contributions of this paper are outlined in the following:

Sizing and operation of community energy storage for a multi-interval local market: In addition to determining the local prices, the aggregator can offer new services to the community through a centralized battery storage. The storage can be used for peak shaving during periods of high demand or reducing the interaction with the grid; hence, lower cost and higher self-sufficiency for the prosumers [33]. Despite being an essential element for business viability, optimal planning of community storage for maximizing the revenue of aggregators remains understudied. In this regard, we aim to size the community storage within a local market considering load demand response and the interaction between the aggregator and prosumers. When the optimal capacity of community storage is determined, the daily battery operation is scheduled so as to avoid calendar aging when the battery sits idle, while maximizing the aggregator profit.

Market operation using two pricing schemes: Since the aggregator, who holds financial interests, functions as a central entity, it is not impartial in the local market. Thus, it may undermine the nature of local trading; hence preventing prosumers from achieving their true benefits. To address this issue, we structure the local market such that the aggregator's pricing is always more attractive to the participating prosumers than the reference prices offered by retailers. We also demonstrate two different pricing schemes, as two business models for the aggregator, to represent the trade-off between the aggregator's profit and prosumers' utility.

Inter-temporal rebound effect of prosumers: One important aspect that must be governed is the energy management of the participating prosumers. Since more than 90% of the electrical appliances at the residential premises are shiftable loads [44], the inter-temporal demand flexibility must be taken into account during price determination by the aggregator. Demand flexibility in this paper is a lump sum quantity. This allows the aggregator to see when the prosumers are most active at home (high energy consumption), and thus, have higher flexibility to offer. Moreover, the prosumers' privacy is respected due to the consideration of a lump sum quantity without knowing the details of any specific household equipment. This way, the amount of flexibility will be decided by the local energy management system at the prosumers' end. Therefore, at the end of the time horizon, total adjusted demand must remain the same as the initial total expected consumption for every prosumer. To capture the price-responsiveness of prosumers, a piecewise linear function is used to model their demand response.

The remaining of the paper is structured as follow. Section 2 presents a comprehensive literature review about electricity local markets. Section 3 explains the aggregator model based on the proposed market structure, both conceptually and mathematically. The optimization formulation for both the optimal battery capacity sizing and market operation are discussed in Section 4. In Section 5, we propose the method for recasting the bilevel problem into a mixed-integer linear programming (MILP) model. The numerical results of implementing the model using the real-world data are presented in Section 6. Finally, the paper is concluded in Section 7.

2 RELATED WORK

Due to the recent advances in smart grid technology, local trading schemes have gained significant interest in the energy sector, e.g., in the community microgrid management and operation [5, 6]. The concept is motivated by the microgeneration and local consumption of energy at the edge of the distribution network [16]. From the prosumers' viewpoint, local trading helps reduce the cost of electricity consumption [23] and earn profit by selling excess generation at higher prices than the FiTs [28]. From the power system operator perspective, the benefits include local generation and demand balance in the network [29] and facilitating a larger DER deployment [28]. Also, the emission of greenhouse gases is expected to reduce by promoting the local consumption and production [39]. However, most of the existing research studies focused on the single-interval market operation by ignoring the time-coupling nature of shiftable loads [7, 25, 26]. Other papers investigated the load rebound effect by solving the market with 24-hour lookahead, but with a fixed price assumption making it difficult to fully maximise the market surplus [13]. The recent work of Werner *et al.* considers the time-coupling nature of load shifting in all periods [46]. However, the prosumers' price-responsiveness was ignored, while the overall comfort was maintained by meeting the expected demand at all times. Our model is motivated by the same concept of multi-interval market dispatch but also considers the satisfaction of prosumers from consuming electricity at every time interval.

Pricing structure within a local market has mostly centered around two main schemes: a two-price market for purchase and sale of electricity [3, 26], or one consensus price for both buyers and sellers [19, 46]. While the former group resembles the current retail structure, where there are separate tariffs for buying and selling energy [24], the latter pricing scheme loosely represents 'wholesale prices' such that buying prices are equal to selling prices [31, 32]. However, the profit analysis between both schemes was not clear for the market participants. Hence, in this paper, we want to analyze the quantitative profits and utility in both pricing schemes for the aggregator and prosumers, respectively. Then, depending on the strategy of the aggregator, it can either choose a business model that maximizes their profit or attract more customers with the business model that gives higher utility for prosumers.

Technology optimal sizing has gained significant interest in several contexts, including solar PV [18, 47] and battery storage systems [4, 40]. However, most of these works are limited to a single household [40] or aim to meet the anticipated consumption at a minimum storage capacity [22]. Wang and Huang [45] proposed a microgrid framework for distributed battery systems to support the energy trading. Whereas the work of [25] adopted a centralized storage unit with the capability of performing energy arbitrage to maximize the profit of the market operator. However, they considered a fixed battery capacity by eliminating the impact of the prosumers response. In [8], the authors developed a sizing algorithm for a community-level storage considering initial acquisition cost, maintenance and future replacement. However, similar to [13], the model assumes a fixed price of electricity for the market participants, where the comfort of prosumers is not considered when deviating from the base load. In our model, however, we determine the optimal battery size while considering the prosumers' utility with the integration of dynamic pricing for the proposed multi-interval local market.

3 PROBLEM STATEMENT

Since we are trying to maximize the profit of all participating parties, constructing a good pricing scheme is crucial for attracting new customers and exploting maximum available flexibility. In our setup, the market aggregator is responsible for price determination while serving as an intermediary entity that operates the local market. The aggregator must always provide the prosumers with improved prices over conventional retailers. Such lucrative prices can be in the form of lower buying prices or higher FiT for excess solar generation. These new prices motivate prosumers to alter their consumption from the expected demand based on their utility function. In addition, the nature of shiftable loads requires the aggregator to consider the time-coupling rebound effect during the price determination. This means that during on-peak hours, the aggregator can increase selling prices to lower the prosumers' demand so that they can sell more energy. Also, the aggregator can reduce buying prices during the intervals of surplus generation to motivate more electricity consumption. This interplay between the two prices allows the total expected demand to remain unchanged at the end of the day with respect to the rebound effect constraint.

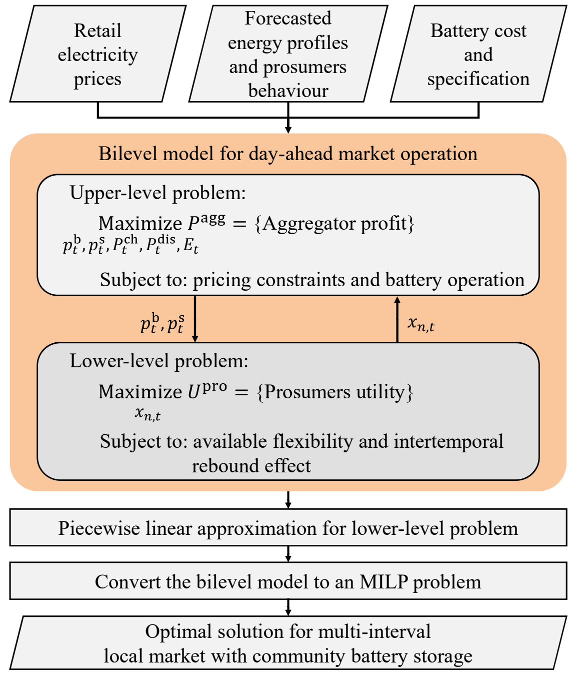

Figure 1: Bi-level model for day-ahead local market operation

This sequential movement between an aggregator and prosumers represents a hierarchical structure of a strategic game. Since both the aggregator and prosumers are aiming at maximizing their objective functions with conflicting interests, the problem is an instance of the Stackelberg game, which can be formulated as a bilevel program. In this game, the aggregator is the leader determining the trading prices for the local market. The followers are prosumers, who are considered rational via the administration of a home energy management system (HEMS). Given the aggregator's prices, the prosumers will adjust their consumption in regard to their utility function. This process is shown in Figure 1. It can be seen in the figure that the market prices, p_t^{b} and p_t^{s}, obtained from solving the aggregator's maximization problem are passed to the prosumers' problem. Thus, they are deemed as decision variables for the leader while being considered as known parameters for the followers. Conversely, in the lower level, each prosumer maximizes their interest by optimizing the consumption. Hence, the adjusted demand, $x_{n,t}$, are decision variables for the lower level, while known at the upper level problem. Together with the local prices, the aggregator needs to determine the charging and discharging power, P_t^{ch} and P_t^{dis}, for the community battery state-of-charge (SOC) E_t, to maximize its profit.

The bilevel problem can be solved by reformulating it as a Mathematical Program with Equilibrium Constraint (MPEC) [30]. In such problems, the Karush-Kuhn-Tucker (KKT) optimality conditions are typically used to replace the lower level problem with a set of constraints for the upper level. However, the converted single-level optimization is non-convex, which is not only intractable but also does not guarantee convergence to optimality. To resolve the issue, we firstly apply a piecewise approximation to the non-linear terms in the prosumers objective function. Then, we apply the strong duality theorem to obtain the equivalent linear expression in the final optimization model. The outcome is a single-level MILP problem, which guarantees the convergence to the optimal solution.

The physical implementation of the proposed local market requires a bi-directional communication link between the aggregator and the participating prosumers. The local market interacts with the upstream utility grid to balance any mismatch in the local generation and demand. Moreover, each prosumer must be equipped with a HEMS that can autonomously schedule the household appliances based on the preferences of the dwellers. All HEMS within the same community must be integrated with a homogeneous trading algorithm as a representative of a rational player. From the load schedule ability and the historical data, HEMS is also responsible for predicting and measuring generation, consumption and energy transaction through a smart meter. As the prediction is outside the scope of this paper, it is assumed available in the simulation studies.

4 PROBLEM FORMULATION

In this section, we elaborate on the specific objective functions and constraints of the stakeholders in the proposed bilevel model. The problems are formulated to maximize the profit and utility of the aggregator and the prosumers, respectively. In the battery sizing problem, we maximize the aggregator's profit and operate the battery by considering the cost per energy throughput on daily operation. Upon obtaining the optimal capacity, the sizing problem is modified to schedule the daily operation of local market aiming at fully utilizing the battery potential. Using this bilevel model for local market operation, we determine the local cleared prices.

4.1 Prosumers' role identification

The set of prosumers participating in the local market is denoted by $\mathcal{N} = \{1, 2, ..., N\}$ and $N = |\mathcal{N}|$ is the number of prosumers. Each prosumer $n \in \mathcal{N}$ can produce energy $G_{n,t}$ or consume energy $x_{n,t}$ in each interval $t \in \mathcal{T} = \{1, 2, ..., T\}$. Because each prosumer can either be a buyer or a seller at each time interval depending on their predicted demand $\hat{x}_{n,t}$ and solar generation $G_{n,t}$, their roles must be identified before the trading. These roles are reflected in the buying/selling prices within the local market, $p_{n,t}$, and the buying/selling prices from the retailer, $\lambda_{n,t}$. If buyer is the role, the prosumer is exposed to the buying prices from the local market as $p_{n,t} = p_t^{\text{b}}$, and the utility grid as $\lambda_{n,t} = \lambda_t^{\text{res,b}}$. Whereas sellers are the opposite of buyers, i.e., $p_{n,t} = p_t^{\text{s}}$ and $\lambda_{n,t} = \lambda_t^{\text{res,s}}$.

4.2 Aggregator's profit with sizing problem (upper level)

In the proposed setup, the aggregator is sitting between the existing retailer and all the participating prosumers. Any energy transaction within the local market must be accomplished by the intermediary entity. Thus, it is responsible for supplying electricity to all the buyers and purchasing the surplus generation from all the market sellers at interval t. The mismatch between the local community's generation and demand can either be compensated by the community storage or by trading with the conventional retailer. The net profit of the aggregator is as follows:

$$P^{\text{agg}} = \sum_{t\in\mathcal{T}}\sum_{n\in\mathcal{N}}\left[p_{n,t}(x_{n,t} - G_{n,t})\right] - \sum_{t\in\mathcal{T}}(\lambda_t^{\text{b}} n_t^+ - \lambda_t^{\text{s}} n_t^-) - \sum_{t\in\mathcal{T}} P_t^{\text{dis}} B^{\text{ThP}} - B^{\text{Sup}} \tag{1}$$

where the difference in the first term, $(x_{n,t} - G_{n,t})$, represents the amount of energy of each prosumer that should be traded with the aggregator at price $p_{n,t}$. The second term defines the interaction with the upstream grid to balance the local generation and demand mismatch. If the aggregate net energy is positive, the aggregator must procure electricity, n_t^+, at the commercial retail price λ_t^{b}. Conversely, if there is excess generation locally, the aggregator can sell surplus energy, n_t^-, at the FiT, λ_t^{s}. Since the aggregator is considered as a commercial company (large consumer), they are exposed to business retail prices, $\lambda_t^{\text{b}}/\lambda_t^{\text{s}}$, which are different from the residential rates, $\lambda_t^{\text{res,b}}/\lambda_t^{\text{res,s}}$. Please note that the aggregator cannot buy from and sell to the conventional retailer at the same time. This is always ensured because the retailer's sale price is higher than the FiT, thus, only one of the two variables, n_t^+ and n_t^-, would have a non-zero value in each interval. The third term models the battery degradation by applying a per unit cost, B^{ThP}, on the amount of energy discharged from the battery, P_t^{dis}. Assuming that the battery will require replacement once it reaches the total throughput according to the manufacturers' warranty terms, the cost per-kWh is defined as $B^{\text{ThP}} = \frac{B_{\text{Bat}}}{L\cdot\Gamma}$, where B_{Bat} is the battery cost, L is its life time throughput limit, and Γ is the round-trip efficiency. The last term in equation (1) denotes the daily supply charge, B^{Sup}, that the aggregator must pay to the Distribution System Operator for utilizing the network.

4.3 Utility model of prosumers (lower level)

At every interval, prosumers can increase or decrease their satisfaction of consuming electricity by varying their consumption according to the buying/selling prices. Thus, the utility function of the prosumers includes the overall cost of electricity consumption as well as the satisfaction it brings.

$$U^{\text{pro}} = \sum_{t\in\mathcal{T}}\sum_{n\in\mathcal{N}}\left[p_{n,t}(G_{n,t} - x_{n,t}) + B(x_{n,t})\right] \tag{2a}$$

$$B(x_{n,t}) = \lambda_{n,t}(x_{n,t} - \hat{x}_{n,t})\left(1 - \beta_n \frac{x_{n,t} - \hat{x}_{n,t}}{2\hat{x}_{n,t}}\right) \tag{2b}$$

where the first term in (2a) represents the overall cost of electricity for prosumer n. If the net generation, $G_{n,t} - x_{n,t}$, is positive, prosumer n is selling to the aggregator at price $p_{n,t} = p_t^{\text{s}}$ at interval t, whereas prosumer n must buy electricity at price $p_{n,t} = p_t^{\text{b}}$ from the aggregator if the net generation is negative. The second term is the satisfaction of consuming electricity, as expressed by the quadratic function in (2b) introduced by [41]. From the prosumer satisfaction model, it can be seen that the response of the load demand depends on various factors, namely time of the day, retail prices, expected consumption, and a price-responsive parameter depicting prosumers flexibility with respect to prices, i.e., β_n $(0 < \beta_n < 1)$.

$\beta_n = 0$ means that prosumer n is 100% flexible at time t at the given electricity price; hence, load can be at the baseline or at the maximum expected demand in that time. This parameter can either be reported by the prosumers during the configuration of HEMS or estimated by the aggregator over time [1, 36]. Moreover, the quadratic satisfaction function in (2b) is an ascending concave function; hence, the higher the consumption, the higher the satisfaction value of the prosumers. However, extra consumption increases the electricity bill of the prosumers. Therefore, the competing nature of the two terms requires the prosumers to make rational decision with respect to the prices of the aggregator.

4.4 Community-level battery sizing problem

To represent the hierarchical decision-making process among the market stakeholders, Stackelberg game theory is employed in the local market model. In addition to setting the local prices for the bilevel program, the aggregator must also efficiently operate the community-level battery unit by determining the optimal storage capacity and by scheduling charging/discharging of the storage unit in each interval. The bilevel model for the aggregator's community battery sizing problem is formulated as follows:

$$\max_{\mathbf{\Psi_1}} P^{\text{agg}} = \sum_{t\in\mathcal{T}}\sum_{n\in\mathcal{N}}\left[p_{n,t}(x_{n,t}-G_{n,t})\right] - \sum_{t\in\mathcal{T}}(\lambda_t^{\text{b}}n_t^{+} - \lambda_t^{\text{s}}n_t^{-}) - \sum_{t\in\mathcal{T}}P_t^{\text{dis}}B^{\text{ThP}} - B^{\text{Sup}} - B_{\text{Bat}}^{\text{Pen}} \tag{3a}$$

s.t.

$$\lambda_t^{\text{res,s}} \le p_t^{\text{s}} \le p_t^{\text{b}} \le \lambda_t^{\text{res,b}} \quad \forall t\in\mathcal{T} \tag{3b}$$

$$\sum_{n\in\mathcal{N}}(x_{n,t}-G_{n,t}) + P_t = n_t^{+} - n_t^{-} \quad \forall t\in\mathcal{T} \tag{3c}$$

$$E_t = E^{\text{init}} - \frac{1}{\Gamma}\sum_{j=1}^{t}P_t^{\text{dis}} + \sum_{j=1}^{t}P_t^{\text{ch}} \quad \forall t\in\mathcal{T} \tag{3d}$$

$$\underline{\text{SOC}}\,E^{\text{cap}} \le E_t \le \overline{\text{SOC}}\,E^{\text{cap}} \quad \forall t\in\mathcal{T} \tag{3e}$$

$$P_t = P_t^{\text{ch}} - P_t^{\text{dis}} \quad \forall t\in\mathcal{T} \tag{3f}$$

$$P^{\min} \le P_t \le P^{\max} \quad \forall t\in\mathcal{T} \tag{3g}$$

$$P^{\max} = -P^{\min} = \frac{E^{\text{cap}}}{T_c} \tag{3h}$$

$$P_t - P_{t-1} = \delta_t^{+} - \delta_t^{-} \quad \forall t\in\mathcal{T}, t>0 \tag{3i}$$

$$B_{\text{Bat}}^{\text{Pen}} = \frac{1}{M}(E^{\text{cap}} + \sum_{t\in\mathcal{T}}\delta_t^{+} + \sum_{t\in\mathcal{T}}\delta_t^{-}) \tag{3j}$$

$$\max_{x_{n,t}} U^{\text{pro}} = \sum_{t\in\mathcal{T}}\sum_{n\in\mathcal{N}}\left[p_{n,t}(G_{n,t}-x_{n,t}) + B(x_{n,t})\right] \tag{3k}$$

s.t.

$$x_{n,t}^{\min} \le x_{n,t} \le x_{n,t}^{\max} \quad \forall n\in\mathcal{N},\ \forall t\in\mathcal{T} \tag{3l}$$

$$\sum_{t\in\mathcal{T}}x_{n,t} = \sum_{t\in\mathcal{T}}\hat{x}_{n,t} \quad \forall n\in\mathcal{N} \tag{3m}$$

where $\mathbf{\Psi_1} = \{p_t^{\text{b}}, p_t^{\text{s}}, P_t^{\text{ch}}, P_t^{\text{dis}}, E_t, n_t^{+}, n_t^{-}, \delta_t^{+}, \delta_t^{-}, x_{n,t}\}$. The upper level program (3a)–(3j) maximizes the aggregator's profit from coordinating the local transactions. The newly added term in (3a), $B_{\text{Bat}}^{\text{Pen}}$, represents a small penalty for sizing and operating the community battery which is defined in equations (3i) and (3j). To be specific, when solving for the sizing optimization, the battery capacity, E^{cap}, can take on any arbitrarily large value as long as it can satisfy the charging and discharging requirements in each interval. Thus, a penalty coefficient, $\frac{1}{M}$ where M is a sufficiently large number, is applied to lower the maximum capacity to a value that is equal to highest battery SOC at any given time. Please note that the battery investment cost is already reflected in the per-unit cost, B^{ThP}. In addition, the battery operation can fluctuate rapidly from one interval to the next that is harmful to the battery lifetime. Hence, it is necessary to reduce switching from charging to discharging, δ^{-}, and vice versa, δ^{+}, by considering the charging/discharging sequences in consecutive intervals (3i), and penalizing it (3j). To ensure that the local market always provides more incentives than the conventional retailer, the local prices are constrained by (3b). Equation (3c) denotes the local net demand from the aggregated energy profiles of all the prosumers and the battery operation, P_t. At any time interval, the battery SOC is given in (3d) with a lower ($\underline{\text{SOC}}$) and upper ($\overline{\text{SOC}}$) bounds in (3e). Please bear in mind that due to the round-trip efficiency, Γ, and the cost per energy throughput, it is guaranteed that at most only one of the two charging, P_t^{ch}, and discharging, P_t^{dis}, variables in (3f) can be positive. The limits on charging and discharging power are presented in (3g) and (3h), where the constant T_c is the minimum hours required to fully charge the battery from the lowest SOC, and is given by the manufacturers when purchasing from the available models in the market, e.g., Tesla PowerWall [43].

In the lower level optimization (3k)–(3m), the objective is to maximize the prosumers utility over the time horizon. In this model, the HEMS predicts day-ahead PV generation and load demand. The expected energy consumption for every interval $\hat{x}_{n,t}$ for one day ahead consists of base load and flexible demand. The flexible demand allows prosumers to vary their consumption either upwards or downwards to minimize their electricity costs. Correspondingly, this component specify boundaries on the energy demand in (3l). The lower bound $x_{n,t}^{\min} = (1-\alpha_{n,t})\hat{x}_{n,t}$ is considered as the base load that must always be delivered, whereas the upper bound $x_{n,t}^{\max} = (1+\alpha_{n,t})\hat{x}_{n,t}$ is the maximum demand that can be shifted to that interval. To determine the amount of flexible demand at each interval, a weighting ratio on the expected consumption, i.e. $\alpha_{n,t}(0 < \alpha_{n,t} < 1)$, is utilized. Depending on the aggregator's prices, prosumers can decide to deviate from their expected demand to maintain their utility at the highest value. However, at the end of the time horizon, the adjusted consumption must always be equal to the expected demand, which is ensured in (3m). This time-coupling demand constraint represents the inter-temporal rebound effect of the prosumers.

4.5 Market operation problem

During the market operation, the battery capacity is already determined. Although the proposed sizing problem can still be used for clearing the market, the model cannot use the full potential of the battery. This is due to the fact that the battery operation is restricted by the cost per throughput, B^{ThP}, which causes the battery to stay idle when the market price drops below the per-unit throughput cost. Since manufacturers normally offer their storage warranty based on the number of years since the installation or the total aggregated throughput, whichever comes first, the battery might not achieve its rated cycle count before reaching the end of warranty period. The issue can be tackled by removing the cost per throughput and allowing the battery to freely operate on a daily basis. However, due to the nature of ToU pricing, the storage will be forced to practice tariff arbitrage by purchasing and selling at different price ranges. This is not economical since the battery operation is usually costlier than tariff arbitrage; hence, leading to faster degradation by performing multiple cycles per day. As a result, the proposed solution is to allow the battery an amount of free throughput for daily operation and apply the per-unit cost on the extra throughput within a day. The daily free throughput, $C^{\text{ThP}} = \frac{L\cdot\Gamma}{W_{\text{Pe}}}$, is calculated from the lifetime throughput, $L \cdot \Gamma$, and the warranty period, W_{Pe}, that are specified by the manufacturers. In this respect, the battery sizing problem, (3), can be modified to be used for optimal daily operation of the local market as follows:

$$\max_{\Psi_2} P^{\text{agg}} = \sum_{t\in\mathcal{T}}\sum_{n\in\mathcal{N}} \left[p_{n,t}(x_{n,t} - G_{n,t})\right] - \sum_{t\in\mathcal{T}}(\lambda_t^{\text{b}} n_t^+ - \lambda_t^{\text{s}} n_t^-)$$
$$- \Big(\sum_{t\in\mathcal{T}} P_t^{\text{dis}} - C^{\text{ThP}}\Big) B^{\text{ThP}} \cdot \phi^{\text{ThP}} - B^{\text{Sup}} - B_{\text{Bat}}^{\prime\text{Pen}} \tag{4a}$$

s.t. (3a)–(3i), (3k)–(3m) (4b)

$$B_{\text{Bat}}^{\prime\text{Pen}} = \frac{1}{M}\Big(\sum_{t\in\mathcal{T}} \delta_t^+ + \sum_{t\in\mathcal{T}} \delta_t^-\Big) \tag{4c}$$

$$-M(1-\phi^{\text{ThP}}) \leq \sum_{t\in\mathcal{T}} P_t^{\text{dis}} - C^{\text{ThP}} \leq M \cdot \phi^{\text{ThP}} \tag{4d}$$

$$\phi^{\text{ThP}} \in \{0,1\} \tag{4e}$$

where $\Psi_2 = \{p_t^{\text{b}}, p_t^{\text{s}}, P_t^{\text{ch}}, P_t^{\text{dis}}, E_t, n_t^+, n_t^-, \delta_t^+, \delta_t^-, \phi^{\text{ThP}}, x_{n,t}\}$. The penalty term, $B_{\text{Bat}}^{\prime\text{Pen}}$, in (4c) is modified to eliminate the battery capacity, which is known at this stage. A new binary variable, ϕ^{ThP}, is introduced to determine whether the battery used more than the provided throughput for that day. Constraints (4d) enforce a value of 0 on ϕ^{ThP} if the discharge energy is within the limit while set it to 1 if the limit is reached; hence, the corresponding cost is applied to the aggregator, as noted in (4a). It is worth noting that the aggregator's profit, i.e., the objective function (4a), does not include the initial battery cost. This cost is then considered as daily payment and is deducted from the objective value when analyzing the aggregator's net profit in subsection 6.2.

5 SOLUTION METHOD

The proposed bilevel problem can be solved by deriving the KKT optimality conditions for the lower level problem, which turns the optimization into a single-level model [11]. However, this conversion introduces new complementarity constraints and combines all the decision variables from both levels. Although the complementarity constraints can be linearized using binary variables [15], there will be bilinear terms that include multiplication of the load consumption, $x_{n,t}$, and the local prices, $p_{n,t}$, in (3a) making the whole problem to be non-convex. To address the issue, strong duality theorem [10] can be applied to obtain a linear expression equal to the bilinear term, $p_{n,t}x_{n,t}$. However, since the satisfaction function in the lower level is quadratic, its dual function will also introduce new bilinear terms in the model. Therefore, the satisfaction needs to be linearized too. In this regard, the workflow for solving the bilevel model is as follows:

(1) **Step 1**: Apply piecewise linear approximation on the satisfaction function. Since the satisfaction function is concave with respect to the decision variable, $x_{n,t}$, (see expression in Appendix A), no binary variables are required.
(2) **Step 2**: Apply strong duality theorem on the lower level problem to obtain the equivalent linear expression for $p_{n,t}x_{n,t}$.
(3) **Step 3**: Substitute the lower level problem by KKT optimality conditions to cast the bilevel program into an MPEC problem.

5.1 Step 1: Linearization of the lower level problem

To facilitate the understanding of readers, the linearization approximation of a concave function $f(x)$ into different regions $||\text{PW}||$ over the range $[x^{\min}, x^{\max}]$ is expressed in Appendix B. Since it is assumed that the lower and upper bounds of the flexibility is symmetric over the predicted load demand, the number of segments $||\text{PW}||$ must be even to enforce a change of slope at the forecast consumption point. The optimization formulation is then written as follows with the succession of dual variables for each constraint equation.

$$\max_{x_{n,t}, x_{n,t}^{pw}} U^{\text{pro}} = \sum_{t\in\mathcal{T}}\sum_{n\in\mathcal{N}} \Bigg[B(x_{n,t}^{\min}) + \sum_{pw\in\text{PW}} M_{n,t}^{pw} x_{n,t}^{pw}$$
$$+ p_{n,t}(G_{n,t} - x_{n,t})\Bigg] \tag{5a}$$

s.t.

$$x_{n,t} = x_{n,t}^{\min} + \sum_{pw\in\text{PW}} x_{n,t}^{pw} : \gamma_{n,t} \quad \forall n \in \mathcal{N},\ \forall t \in \mathcal{T} \tag{5b}$$

$$0 \leq x_{n,t}^{pw} \leq \frac{x_{n,t}^{\max} - x_{n,t}^{\min}}{||\text{PW}||} : \mu_{n,t}^{pw,1}, \mu_{n,t}^{pw,2}$$
$$\forall pw \in \text{PW},\ \forall \text{n} \in \mathcal{N},\ \forall \text{t} \in \mathcal{T} \tag{5c}$$

$$\sum_{t\in\mathcal{T}} x_{n,t} = \sum_{t\in\mathcal{T}} \hat{x}_{n,t} : \varphi_n \quad \forall n \in \mathcal{N}. \tag{5d}$$

5.2 Step 2: Linearization of the bilinear terms

With the approximation of the satisfaction function, the lower level problem is linear and continuous. The strong duality theorem can be used to obtain the equivalent expression of $p_{n,t}x_{n,t}$ at the optimum. At such point, the values for both the primary (5a) and its dual objective function are equal to each other [10]:

$$\sum_{t\in\mathcal{T}}\sum_{n\in\mathcal{N}}\left[B(x_{n,t}^{\min})+\sum_{pw\in\text{PW}}M_{n,t}^{pw}x_{n,t}^{pw}+p_{n,t}(G_{n,t}-x_{n,t})\right]=$$
$$\sum_{t\in\mathcal{T}}\sum_{n\in\mathcal{N}}\Bigg[B(x_{n,t}^{\min})+p_{n,t}G_{n,t}+x_{n,t}^{\min}\gamma_{n,t}+\sum_{pw\in\text{PW}}\frac{x_{n,t}^{\max}-x_{n,t}^{\min}}{||\text{PW}||}\mu_{n,t}^{pw,2}+\hat{x}_{n,t}\varphi_n\Bigg]. \tag{6}$$

Then, the final model can be cast into an MILP by replacing the bilinear terms $p_{n,t}x_{n,t}$ with their equivalent linear expressions:

$$\sum_{t\in\mathcal{T}}\sum_{n\in\mathcal{N}}p_{n,t}x_{n,t}=\sum_{t\in\mathcal{T}}\sum_{n\in\mathcal{N}}\Bigg[-x_{n,t}^{\min}\gamma_{n,t}-\hat{x}_{n,t}\varphi_n+\sum_{pw\in\text{PW}}\left(M_{n,t}^{pw}x_{n,t}^{pw}-\frac{x_{n,t}^{\max}-x_{n,t}^{\min}}{||\text{PW}||}\mu_{n,t}^{pw,2}\right)\Bigg]. \tag{7}$$

5.3 Step 3: Casting the bilevel problem into an MILP model

The final step in solving the proposed bilevel problem is casting it into an MPEC model. The linearized lower level problem (5a)–(5d) is substituted by the KKT optimality conditions as follows:

$$p_{n,t}+\gamma_{n,t}+\varphi_n=0\quad\forall n\in\mathcal{N},\ \forall t\in\mathcal{T} \tag{8a}$$

$$M_{n,t}^{pw}+\gamma_{n,t}+\mu_{n,t}^{pw,1}-\mu_{n,t}^{pw,2}=0\quad\forall pw\in\text{PW},\ \forall\text{n}\in\mathcal{N},\ \forall\text{t}\in\mathcal{T} \tag{8b}$$

$$x_{n,t}-x_{n,t}^{\min}-\sum_{pw\in\text{PW}}x_{n,t}^{pw}=0\quad\forall n\in\mathcal{N},\ \forall t\in\mathcal{T} \tag{8c}$$

$$\sum_{t\in\mathcal{T}}x_{n,t}-\sum_{t\in\mathcal{T}}\hat{x}_{n,t}=0\quad\forall n\in\mathcal{N} \tag{8d}$$

$$x_{n,t}^{pw}\geq 0\quad\forall pw\in\text{PW},\ \forall\text{n}\in\mathcal{N},\ \forall\text{t}\in\mathcal{T} \tag{8e}$$

$$\frac{x_{n,t}^{\max}-x_{n,t}^{\min}}{||\text{PW}||}-x_{n,t}^{pw}\geq 0\quad\forall pw\in\text{PW},\ \forall\text{n}\in\mathcal{N},\ \forall\text{t}\in\mathcal{T} \tag{8f}$$

$$\mu_{n,t}^{pw,1},\mu_{n,t}^{pw,1}\geq 0\quad\forall pw\in\text{PW},\ \forall\text{n}\in\mathcal{N},\ \forall\text{t}\in\mathcal{T} \tag{8g}$$

$$x_{n,t}^{pw}\leq\Phi_{n,t}^{pw,1}M\quad\forall pw\in\text{PW},\ \forall\text{n}\in\mathcal{N},\ \forall\text{t}\in\mathcal{T} \tag{8h}$$

$$\frac{x_{n,t}^{\max}-x_{n,t}^{\min}}{||\text{PW}||}-x_{n,t}^{pw}\leq\Phi_{n,t}^{pw,2}M\quad\forall pw\in\text{PW},\ \forall\text{n}\in\mathcal{N},\ \forall\text{t}\in\mathcal{T} \tag{8i}$$

$$\mu_{n,t}^{pw,1}\leq(1-\Phi_{n,t}^{pw,1})M\quad\forall pw\in\text{PW},\ \forall\text{n}\in\mathcal{N},\ \forall\text{t}\in\mathcal{T} \tag{8j}$$

$$\mu_{n,t}^{pw,2}\leq(1-\Phi_{n,t}^{pw,2})M\quad\forall pw\in\text{PW},\ \forall\text{n}\in\mathcal{N},\ \forall\text{t}\in\mathcal{T} \tag{8k}$$

$$\Phi_{n,t}^{pw,1},\Phi_{n,t}^{pw,2}\in\{0,1\}\quad\forall pw\in\text{PW},\ \forall\text{n}\in\mathcal{N},\ \forall\text{t}\in\mathcal{T} \tag{8l}$$

where (8a)–(8d) are derived from the Lagrangian function and (8e)–(8l) are the equivalent linear expression of the complementarity constraints (see Appendix C). These KKT optimality conditions together with the primal constraints of the upper level problem constitute the feasible region of the final MILP model. Also, the objective function is derived from the upper level problem with the linear substitution for the bilinear terms. The final model of the sizing problem is written as follows:

$$\max_{\mathbf{\Psi_3}}P^{\text{agg}}=\sum_{t\in\mathcal{T}}\sum_{n\in\mathcal{N}}\Bigg[-x_{n,t}^{\min}\gamma_{n,t}-\hat{x}_{n,t}\varphi_n-p_{n,t}G_{n,t}+\sum_{pw\in\text{PW}}\left(M_{n,t}^{pw}x_{n,t}^{pw}-\frac{x_{n,t}^{\max}-x_{n,t}^{\min}}{||\text{PW}||}\mu_{n,t}^{pw,2}\right)\Bigg]-B^{\text{Sup}}-\sum_{t\in\mathcal{T}}(\lambda_t^{\text{b}}n_t^+-\lambda_t^{\text{s}}n_t^-)-\sum_{t\in\mathcal{T}}P_t^{\text{dis}}B^{\text{ThP}}-B_{\text{Bat}}^{\text{Pen}} \tag{9a}$$

$$\text{s.t. (3b)–(3j), (8a)–(8l)} \tag{9b}$$

where $\mathbf{\Psi_3}=\{p_t^{\text{b}},p_t^{\text{s}},P_t^{\text{ch}},P_t^{dis},E_t,n_t^+,n_t^-,\delta_t^+,\delta_t^-,x_{n,t},x_{n,t}^{pw},\gamma_{n,t},\varphi_n,\mu_{n,t}^{pw,1},\mu_{n,t}^{pw,2},\Phi_{n,t}^{pw,1},\Phi_{n,t}^{pw,2}\}$. The market operation problem is presented as follows:

$$\max_{\mathbf{\Psi_4}}P^{\text{agg}}=\sum_{t\in\mathcal{T}}\sum_{n\in\mathcal{N}}\Bigg[-x_{n,t}^{\min}\gamma_{n,t}-\hat{x}_{n,t}\varphi_n-p_{n,t}G_{n,t}+\sum_{pw\in\text{PW}}\left(M_{n,t}^{pw}x_{n,t}^{pw}-\frac{x_{n,t}^{\max}-x_{n,t}^{\min}}{||\text{PW}||}\mu_{n,t}^{pw,2}\right)\Bigg]-B^{\text{Sup}}-\sum_{t\in\mathcal{T}}(\lambda_t^{\text{b}}n_t^+-\lambda_t^{\text{s}}n_t^-)-\left(\sum_{t\in\mathcal{T}}P_t^{\text{dis}}-C^{\text{ThP}}\right)B^{\text{ThP}}\cdot\phi^{\text{ThP}}-B_{\text{Bat}}^{\prime\text{Pen}} \tag{10a}$$

$$\text{s.t. (3b)–(3i), (4c)–(4e), (8a)–(8l)} \tag{10b}$$

where $\mathbf{\Psi_4}=\{p_t^{\text{b}},p_t^{\text{s}},P_t^{\text{ch}},P_t^{\text{dis}},E_t,n_t^+,n_t^-,\delta_t^+,\delta_t^-,x_{n,t},x_{n,t}^{pw},\phi^{\text{ThP}},\gamma_{n,t},\varphi_n,\mu_{n,t}^{pw,1},\mu_{n,t}^{pw,2},\Phi_{n,t}^{pw,1},\Phi_{n,t}^{pw,2}\}$.

6 SIMULATION STUDY

To show the applicability of the proposed local market with centralized battery storage, we use real-world data of East coast Australian prosumers [9]. In subsection 6.1, we present the simulation setup and the workflow for sizing the community storage for both pricing schemes. In subsection 6.2, we highlight the quantitative profits and utility for the aggregator and prosumers, respectively.

6.1 Simulation setup

The load demand database contains one year worth of data for 300 prosumers including gross solar PV generation and general electricity consumption from 2012. Due to the growth in size of the average rooftop solar PV system in Australia [12], we increased the PV generation data for all the prosumers by 2.5 times uniformly and finally picked 33 prosumers with the highest rooftop PV capacity for the simulation. Originally, the data has a resolution of half hour, but to reduce the simulation time, we re-sampled the load demand profiles to hourly intervals. Also, instead of using the whole year worth of data for simulation, we selected the first 3 days of each month (36 days in total) for ease of gathering results and analysis. Out of those 3 days, two days are deliberately picked as working weekdays and the third day is either Saturday or Sunday. Note that

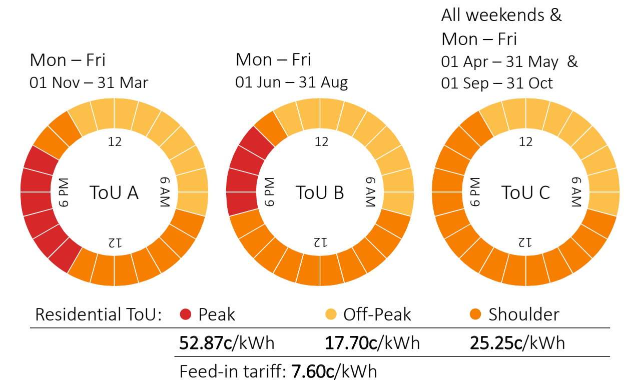

Figure 2: Residential retail ToU from EnergyAustralia [14]

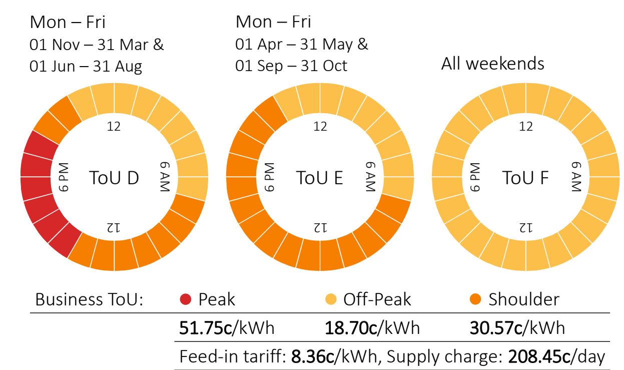

Figure 3: Business retail ToU from EnergyAustralia [14]

the proposed model can be applied for shorter interval resolution as long as appropriate data is available.

EnergyAustralia [14], which is one of the largest electricity retailer in Australia, is chosen as a reference for the retail tariffs in (3b). Since the aggregator is considered as a business consumer, they are subjected to the business plans, which have different prices compared to the residential plans. The overview of the residential and business ToU tariffs from EnergyAustralia is presented in Figure 2 and 3, respectively, with seasonal pricing structure depending

Table 1: Input data for the simulation study

Battery data		
Γ	90	battery round-trip efficiency (%)
$\overline{SOC}$	100	battery maximum SOC (%)
$\underline{SOC}$	0	battery minimum SOC (%)
E^{init}	0	battery initial SOC (kWh)
T_c	2.7	rated energy and power ratio (h)
B^{ThP}	0.23	cost per kWh throughput (AUD$/kWh)
W_{Pe}	10	battery warranty period (years)
L	$E^{cap} \cdot W_{Pe}$	battery warranty kWh throughput (kWh)
Prosumers data		
β_n	0.2	price responsiveness
$\alpha_{n,t}$	0.7	amount of available flexibility (%)

on the months and days of the week. As one can see, the residential electricity plan has a slightly higher on-peak price in comparison with the business plan as opposed to lower rates on the other two periods with a difference of more than 5¢/kWh during the Shoulder periods. As unfavorable as it looks for aggregators in this scenario, they still make profit, as later shown in subsection 6.2, by procuring the energy from local sellers and selling back to the local buyers at higher prices (still lower than retailers' rates). Therefore, this can be a hindrance to attract new customers due to the partiality of the aggregator. To address the issue, we introduce a second pricing scheme by eliminating the gap between buying and selling prices to obtain only one consensus payment in each interval. This is enforced by replacing (3b) with equality constraint such that $\lambda_t^{res,s} \le p_t^s = p_t^b \le \lambda_t^{res,b} \; \forall t \in \mathcal{T}$.

Since the market horizon is 24 hours ahead, the sizing duration is limited to the same horizon with hourly resolution. Although the problem can be optimized for multiple days, the computational time grows exponentially with respect to the number of discrete intervals; hence, intractable. In this regard, the optimal capacity in each day is considered as one of the many candidates that provides us with an optimal range of battery capacities. Different battery sizes within the range are then utilized to rerun the model using the operation formulation in section 4.5. The workflow for determining the optimal storage unit is illustrated in Figure 4.

We use Tesla PowerWall as the battery unit in this study with a cost of AUD$11050 for a 13.5 kWh capacity and 5 kW power rating [43]. Then, the optimal community battery system is constructed by stacking multiple Tesla PowerWalls together to obtain the required capacity and power ratings. Although the battery comes with a default throughput warranty, it is assumed that the community storage can perform at least one cycle per day for 10 years, which is also the warranty period of the unit. This gives the battery a total of 3650 cycles at the end of its life which is lower than the expected warranty term in other works [17, 21]. Moreover, we assumed that the per-unit cost decreases with respect to the scale of the storage system [37]. In this model, the community storage is expected to range between 80 kWh to 300 kWh depending on the number of prosumers. Therefore, we applied an 8% reduction on the battery price. Overall, the cost per kWh throughput is expected to be B^{ThP} = AUD$0.23/kWh. The remaining battery data together with the prosumers input are presented in Table 1. All instances are simulated using Python and Gurobi 9.0 on a desktop with an Intel Core i7 at 2.00GHz CPU and 16GB of RAM.

6.2 The simulation results

The net profit and optimal storage capacities on selected 36 days for both pricing schemes are shown in Figure 5. It is clear that the aggregator receives higher payoff in the two-price scheme by exploiting the gap between the local buying and selling prices. As shown in Figures 2 and 3, both residential and business tariff structures are the same during autumn and spring in Australia (Apr-May and Sep-Oct) with a lower cost for the residential ToU. Hence, the aggregator's net profit is at minimum comparing to summer and winter. Another reason contributing to the low aggregator's profit in those months is the lack of community storage. It can be proven that the battery operation is only economical during

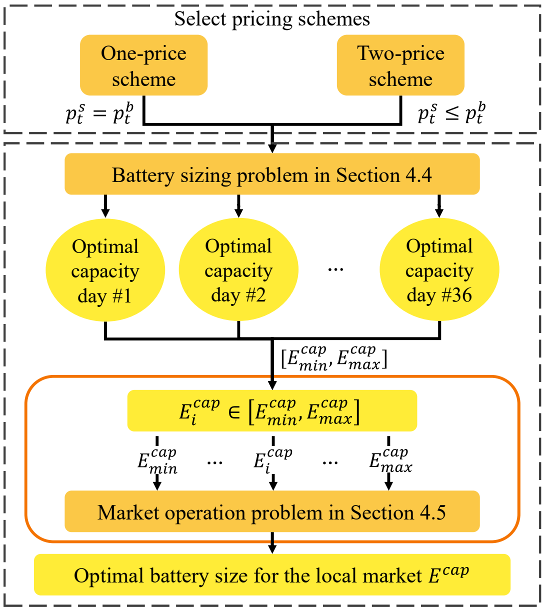

Figure 4: Flowchart for sizing the community battery storage for two pricing schemes

Peak price intervals. To do so, assume that instead of selling excess PV generation back to the grid, the community storage is charged. In that case, the total cost per kWh for the aggregator will tally at 0.3136¢/kWh, which is the sum of the storage cost per kWh throughput and business FiT. This cost is only lower than the Peak tariff and slightly higher than the Shoulder price. Therefore, while the results show different battery sizes for weekdays of winter and summer seasons, it is not cost-effective to adopt a storage unit for the autumn and spring as well as weekends based on the retail tariff structure. The optimal battery results in Figure 5c also reflect the impact of longer summer days and Daylight saving hours in the East coast Australia. Because days are longer in summer, prosumers can generate more electricity from their rooftop PV systems in the early morning and late afternoon when they need energy the most. Thus, less energy is imported during Peak hours, which results in a smaller battery size comparing to the winter months.

As mentioned in subsection 6.1, upon obtaining optimal battery sizes for each day, these values are then used to provide a boundary for finding the single optimal capacity for the entire year. We assume that this community battery is constructed by stacking multiple Tesla PowerWalls together. According to the battery sizes from stage 1, the maximum battery capacity is about 24 Tesla units, which is obtained from a weekday in July where the battery capacity was 322 kWh. Figure 6 shows the net profit from different number of PowerWalls for both pricing schemes. As can be seen, the aggregator's net profits decrease significantly after around 9 Tesla units, we then halve the simulation results to only 12 PowerWalls for ease of observation. The results show that the ideal community storage is six (seven) Tesla PowerWall units in the two (single) pricing scheme. That is equivalent to 81 kWh/30 kW (94.5 kWh/35 kW) in the two (single) pricing scheme. Since the difference

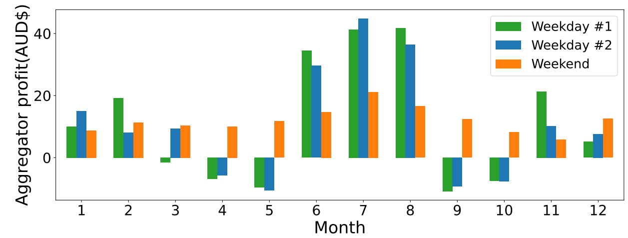

(a) Daily net profit from single pricing scheme

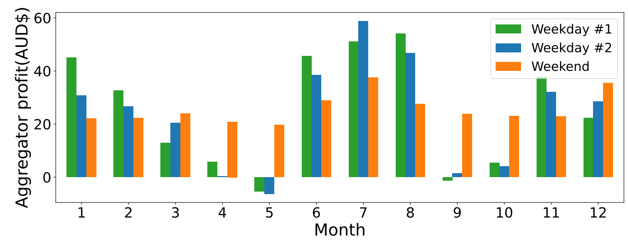

(b) Daily net profit from two pricing scheme

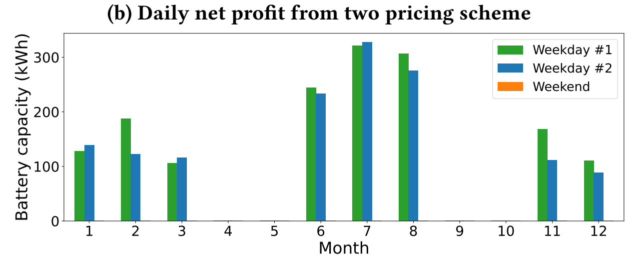

(c) Daily optimal storage capacity

Figure 5: Daily aggregator's net profit and optimal storage capacity from both pricing schemes

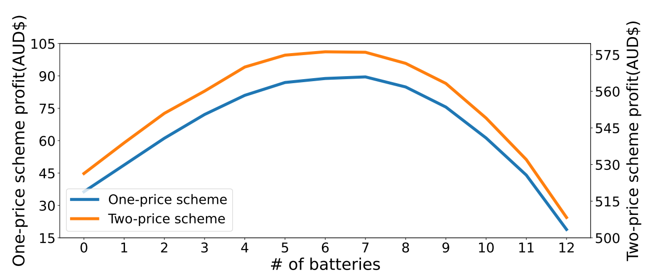

Figure 6: Aggregator's net profit from different number of battery units for both pricing schemes in 36 days

between the profit of six and seven battery units in the one pricing scheme is minimal, we will use six batteries to analyze for the rest of our study. Please note that if a smaller battery step size was considered, the sweep would be less significant in Figure 6. Yet, the optimal battery size would have been between 6 to 7 Powerwalls (81–94.5 kWh) in our case study. If the system is to be scaled up to involve more prosumers, the 13.5 kWh discrete step would be small compared to the optimal size of the battery system; hence, the resolution would be less important. With a maximum profit of AUD$576.16 (AUD$88.8) for the two (single) pricing scheme from the chosen 36 days, a payback period of 5.1 years (8.7 years) can

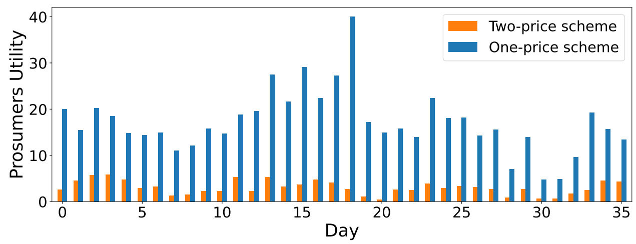

Figure 7: Prosumers' utility in both pricing schemes

be achieved before the battery replacement. Since the aggregator's profit and consumers' utility are competing objectives in this problem, the single pricing scheme, which gives a lower profit to the aggregator, provides much higher utility for prosumers as highlighted in Figure 7. Moreover, when comparing to household-level batteries, the optimal 6 Tesla units are equivalent to 2.45 kWh/0.9 kW storage unit per prosumer, which is significantly less than what prosumers can buy from the market. Even if such a custom-built battery was available, prosumers would not receive the more attractive energy prices offered by the aggregator. Therefore, it is in the best interest of the prosumers to join the local market operated by the aggregator.

The energy and pricing profiles for the market operation utilizing six Tesla battery units are shown in Figure 8 and 9. One weekday and one weekend in December (summer in Australia) are used to highlight the prosumers demand response and community battery operation. In both days, the total net energy profiles show a boost in self-consumption (a decrease in reverse power flow) within the local community, which is achieved by charging the community battery and increasing consumption (shifted loads) from prosumers. Specifically, as shown in Figures 8a and 9a, a cumulative reversed energy of 85.4 kWh is reduced between hours 11–16 for the weekday, while the weekend achieves a reduction of 139.9 kWh between hours 9–16. Then, due to the rebound effect, prosumers reduce their demand in later periods, specifically hours 17–20. These time slots also correspond to the Peak and Shoulder periods of the weekday and weekend, respectively, which is the most profitable intervals for the battery to be discharged. In terms of local prices, it is obvious that the proposed local market always give higher incentives than the conventional retailer in both pricing schemes. Figures 8b and 9b show that in the first six hours of the two days, the local prices are equal to the retailer's prices. Since there is no solar generation, no local trading occurs in these first few intervals. From 9–16, the aggregator decreases the buying prices for the local community in response to the excess solar generation, which triggers higher consumption in prosumers by shifting their load. Then in late afternoon, and also early morning, selling prices are increased from the FiT to incentivize prosumers to lower their consumption with respect to the rebound effect, and to increase utility by selling more energy. As previously mentioned, even though operating the community battery on weekends is not as cost-effective as procuring energy directly from the grid, the battery still performs energy arbitrage due to the free daily throughput in Figure 9c. Also, the weekday profiles of the battery operation in Figure 8c show that

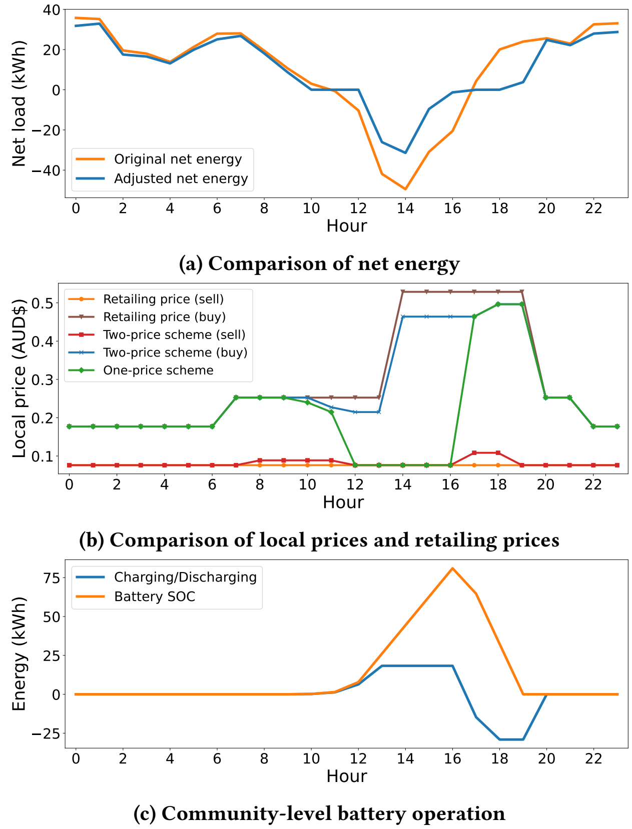

(a) Comparison of net energy

(b) Comparison of local prices and retailing prices

(c) Community-level battery operation

Figure 8: Market operation of a "weekday" in December (summer in Australia) with 81 kWh community battery

the battery does not exceed one cycle per day. Therefore, the aggregator will not fully utilize the battery within the warranty period if it stays idle during weekends.

7 CONCLUSION

In this paper, we proposed a local market model, where the aggregator could optimally size and operate a community-level battery storage system. Since the aggregator was proposed as a central entity that coordinates the energy transaction for the local prosumers, we used Stackelberg game to model the strategic behaviour of the stakeholders. Here, the aggregator took the first move by setting the market prices and battery charging/discharging processes for one day ahead. Then, the local prosumers reacted accordingly by adjusting the energy consumption with respect to their satisfaction and load rebound effect. To solve the sizing problem, the bilevel model was recast into an MILP problem using strong duality theorem and KKT optimality conditions. In the end, two different pricing scenarios were adopted to investigate the trade-off between the aggregator's profit and prosumers' utility. We evaluated the proposed framework using real-world data from 33 prosumers in Australia. The simulation results showed that the local market always provided higher incentives than the conventional retailer, especially in the single pricing scheme. In contrast, the two pricing scheme provided a better business model for the aggregator. Both

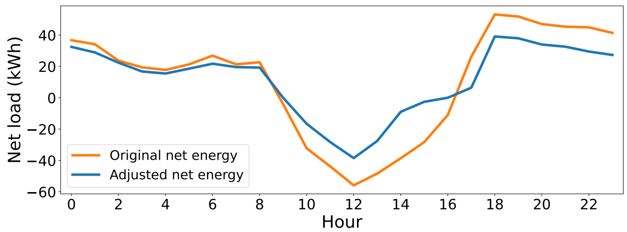

(a) Comparison of net energy

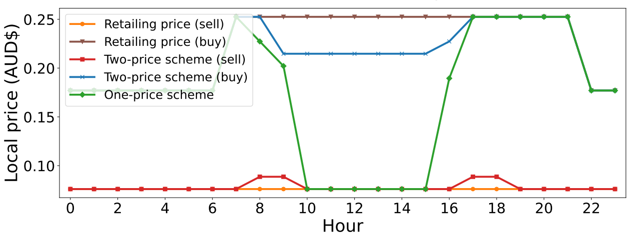

(b) Comparison of local prices and retailing prices

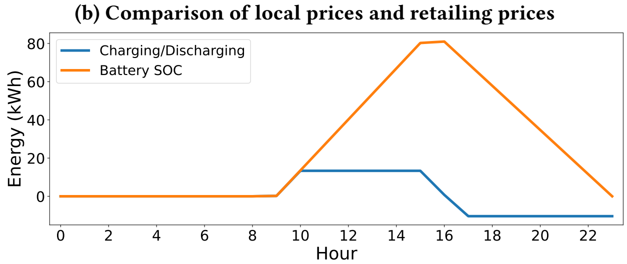

(c) Community-level battery operation

Figure 9: Market operation of a "weekend" in December (summer in Australia) with 81 kWh community battery

pricing schemes were optimal with a 81 kWh/30 kW battery. The future work focuses on comparing the financial benefit of the community storage with multiple household-level battery units, and the improvement of satisfaction function to incorporate the cross elasticity of prosumers responsiveness.

ACKNOWLEDGMENTS

This project is funded jointly by the University of Adelaide industry-PhD grant scheme and Watts A/S, Denmark.

REFERENCES

[1] H.A. Aalami, M. Parsa Moghaddam, and G.R. Yousefi. 2015. Evaluation of nonlinear models for time-based rates demand response programs. *International Journal of Electrical Power & Energy Systems* 65 (2015), 282–290. https://doi.org/10.1016/j.ijepes.2014.10.021

[2] AEMO. 2020. *2020 Electricity Statement of Opportunities for the National Electricity Market.* Technical Report. https://apo.org.au/node/307935

[3] Utkarsha Agwan, Lucas Spangher, William Arnold, Tarang Srivastava, Kameshwar Poolla, and Costas J. Spanos. 2021. Pricing in Prosumer Aggregations Using Reinforcement Learning. In *Proceedings of the Twelfth ACM International Conference on Future Energy Systems* (Virtual Event, Italy) *(e-Energy '21)*. Association for Computing Machinery, New York, NY, USA, 220–224. https://doi.org/10.1145/3447555.3464853

[4] Mohemmed Alhaider and Lingling Fan. 2018. Planning Energy Storage and Photovoltaic Panels for Demand Response With Heating Ventilation and Air Conditioning Systems. *IEEE Transactions on Industrial Informatics* 14, 11 (2018), 5029–5037. https://doi.org/10.1109/TII.2018.2833441

[5] Kelvin Anoh, Dragana Bajovic, Dejan Vukobratovic, Bamidele Adebisi, Dusan Jakovetic, and Mirsad Cosovic. 2018. Distributed Energy Trading with Communication Constraints. In *2018 IEEE PES Innovative Smart Grid Technologies Conference Europe (ISGT-Europe)*. 1–6. https://doi.org/10.1109/ISGTEurope.2018.8571810

[6] Kelvin Anoh, Augustine Ikpehai, Dragana Bajovic, Olamide Jogunola, Bamidele Adebisi, Dejan Vukobratovic, and Mohammad Hammoudeh. 2018. Virtual Microgrids: A Management Concept for Peer-to-Peer Energy Trading *(ICFNDS '18)*. Association for Computing Machinery, New York, NY, USA, Article 43, 5 pages. https://doi.org/10.1145/3231053.3231096

[7] Kelvin Anoh, Sabita Maharjan, Augustine Ikpehai, Yan Zhang, and Bamidele Adebisi. 2020. Energy Peer-to-Peer Trading in Virtual Microgrids in Smart Grids: A Game-Theoretic Approach. *IEEE Transactions on Smart Grid* 11, 2 (2020), 1264–1275. https://doi.org/10.1109/TSG.2019.2934830

[8] Raji Atia and Noboru Yamada. 2016. Sizing and Analysis of Renewable Energy and Battery Systems in Residential Microgrids. *IEEE Transactions on Smart Grid* 7, 3 (2016), 1204–1213. https://doi.org/10.1109/TSG.2016.2519541

[9] Ausgrid. 2012. *Solar home electricity data.* https://www.ausgrid.com.au/Industry/Our-Research/Data-to-share/Solar-home-electricity-data

[10] Stephen Boyd, Stephen P Boyd, and Lieven Vandenberghe. 2004. *Convex optimization.* Cambridge university press.

[11] Enrique Castillo, Antonio J Conejo, Pablo Pedregal, Ricardo Garcia, and Natalia Alguacil. 2011. *Building and solving mathematical programming models in engineering and science.* Vol. 62. John Wiley & Sons.

[12] Australian Energy Council. 2021. *Solar Report Quarter 3, 2021.* Technical Report. https://www.energycouncil.com.au/media/5zylveyr/australian-energy-council-solar-report_q3-2021.pdf

[13] Giulia De Zotti, S. Ali Pourmousavi, Juan M. Morales, Henrik Madsen, and Niels Kjølstad Poulsen. 2019. Consumers' Flexibility Estimation at the TSO Level for Balancing Services. *IEEE Transactions on Power Systems* 34, 3 (2019), 1918–1930. https://doi.org/10.1109/TPWRS.2018.2885933

[14] EnergyAustralia. 2021. *Electricity Retailer.* https://www.energyaustralia.com.au/

[15] José Fortuny-Amat and Bruce McCarl. 1981. A Representation and Economic Interpretation of a Two-Level Programming Problem. *Journal of the Operational Research Society* 32, 9 (01 Sep 1981), 783–792. https://doi.org/10.1057/jors.1981.156

[16] David Gregoratti and Javier Matamoros. 2015. Distributed Energy Trading: The Multiple-Microgrid Case. *IEEE Transactions on Industrial Electronics* 62, 4 (2015), 2551–2559. https://doi.org/10.1109/TIE.2014.2352592

[17] Xuebing Han, Languang Lu, Yuejiu Zheng, Xuning Feng, Zhe Li, Jianqiu Li, and Minggao Ouyang. 2019. A review on the key issues of the lithium ion battery degradation among the whole life cycle. *eTransportation* 1 (2019), 100005. https://doi.org/10.1016/j.etran.2019.100005

[18] Brad Guanqiao Huang, Fiodar Kazhamiaka, and Srinivasan Keshav. 2021. Sizing Solar Panels and Storage for Multiple Roofs. In *Proceedings of the Twelfth ACM International Conference on Future Energy Systems* (Virtual Event, Italy) *(e-Energy '21)*. Association for Computing Machinery, New York, NY, USA, 84–94. https://doi.org/10.1145/3447555.3464858

[19] Yanni Jiang, Kaile Zhou, Xinhui Lu, and Shanlin Yang. 2020. Electricity trading pricing among prosumers with game theory-based model in energy blockchain environment. *Applied Energy* 271 (2020), 115239. https://doi.org/10.1016/j.apenergy.2020.115239

[20] Paul L. Joskow and Catherine D. Wolfram. 2012. Dynamic Pricing of Electricity. *American Economic Review* 102, 3 (May 2012), 381–85. https://doi.org/10.1257/aer.102.3.381

[21] S. Ali Pourmousavi Kani, Phil Wild, and Tapan Kumar Saha. 2020. Improving Predictability of Renewable Generation Through Optimal Battery Sizing. *IEEE Transactions on Sustainable Energy* 11, 1 (2020), 37–47. https://doi.org/10.1109/TSTE.2018.2883424

[22] Fiodar Kazhamiaka, Yashar Ghiassi-Farrokhfal, Srinivasan Keshav, and Catherine Rosenberg. 2019. Comparison of Different Approaches for Solar PV and Storage Sizing. *IEEE Transactions on Sustainable Computing* (2019), 1–1. https://doi.org/10.1109/TSUSC.2019.2946246

[23] Jip Kim and Yury Dvorkin. 2020. A P2P-Dominant Distribution System Architecture. *IEEE Transactions on Power Systems* 35, 4 (2020), 2716–2725. https://doi.org/10.1109/TPWRS.2019.2961330

[24] Guanguan Li, Qiqiang Li, Yi Liu, Huimin Liu, Wen Song, and Ran Ding. 2022. A cooperative Stackelberg game based energy management considering price discrimination and risk assessment. *International Journal of Electrical Power & Energy Systems* 135 (2022), 107461. https://doi.org/10.1016/j.ijepes.2021.107461

[25] Nian Liu, Minyang Cheng, Xinghuo Yu, Jiangxia Zhong, and Jinyong Lei. 2018. Energy-Sharing Provider for PV Prosumer Clusters: A Hybrid Approach Using Stochastic Programming and Stackelberg Game. *IEEE Transactions on Industrial Electronics* 65, 8 (2018), 6740–6750. https://doi.org/10.1109/TIE.2018.2793181

[26] Nian Liu, Xinghuo Yu, Cheng Wang, and Jinjian Wang. 2017. Energy Sharing Management for Microgrids With PV Prosumers: A Stackelberg Game Approach. *IEEE Transactions on Industrial Informatics* 13, 3 (2017), 1088–1098. https://doi.org/10.1109/TII.2017.2654302

[27] Chao Long, Jianzhong Wu, Chenghua Zhang, Meng Cheng, and Ali Al-Wakeel. 2017. Feasibility of Peer-to-Peer Energy Trading in Low Voltage Electrical Distribution Networks. *Energy Procedia* 105 (2017), 2227–2232. https://doi.org/10.1016/j.egypro.2017.03.632 8th International Conference on Applied Energy, ICAE2016, 8-11 October 2016, Beijing, China.

[28] Chao Long, Jianzhong Wu, Chenghua Zhang, Lee Thomas, Meng Cheng, and Nick Jenkins. 2017. Peer-to-peer energy trading in a community microgrid. In *2017 IEEE Power Energy Society General Meeting*. 1–5. https://doi.org/10.1109/PESGM.2017.8274546

[29] Chao Long, Jianzhong Wu, Yue Zhou, and Nick Jenkins. 2018. Peer-to-peer energy sharing through a two-stage aggregated battery control in a community Microgrid. *Applied Energy* 226 (2018), 261–276. https://doi.org/10.1016/j.apenergy.2018.05.097

[30] Zhi-Quan Luo, Jong-Shi Pang, and Daniel Ralph. 1996. *Mathematical programs with equilibrium constraints*. Cambridge University Press.

[31] Chathurika P. Mediwaththe, Marnie Shaw, Saman Halgamuge, David B. Smith, and Paul Scott. 2020. An Incentive-Compatible Energy Trading Framework for Neighborhood Area Networks With Shared Energy Storage. *IEEE Transactions on Sustainable Energy* 11, 1 (2020), 467–476. https://doi.org/10.1109/TSTE.2019.2895387

[32] Chathurika P. Mediwaththe, Edward R. Stephens, David B. Smith, and Anirban Mahanti. 2018. Competitive Energy Trading Framework for Demand-Side Management in Neighborhood Area Networks. *IEEE Transactions on Smart Grid* 9, 5 (2018), 4313–4322. https://doi.org/10.1109/TSG.2017.2654517

[33] Yanfang Mo, Qiulin Lin, Minghua Chen, and Si-Zhao Joe Qin. 2021. Optimal Online Algorithms for Peak-Demand Reduction Maximization with Energy Storage. In *Proceedings of the Twelfth ACM International Conference on Future Energy Systems* (Virtual Event, Italy) *(e-Energy '21)*. Association for Computing Machinery, New York, NY, USA, 73–83. https://doi.org/10.1145/3447555.3464857

[34] SA Power Networks. 2021. *Press Release: SA network sets new mark for solar*. Retrieved January 3, 2022 from https://www.sapowernetworks.com.au/data/311762/press-release-sa-network-sets-new-mark-for-solar/

[35] SA Power Networks. 2021. *Upcoming changes to small embedded generation connections*. Retrieved January 3, 2022 from https://www.sapowernetworks.com.au/data/310548/upcoming-changes-to-small-embedded-generation-connections/

[36] Amir Niromandfam, Ahmad Sadeghi Yazdankhah, and Rasool Kazemzadeh. 2020. Modeling demand response based on utility function considering wind profit maximization in the day-ahead market. *Journal of Cleaner Production* 251 (2020), 119317. https://doi.org/10.1016/j.jclepro.2019.119317

[37] NREL. 2021. *U.S. Solar Photovoltaic System and Energy Storage Cost Benchmarks: Q1 2021*. https://www.nrel.gov/esif/esi-news-202111.html#pubs

[38] Yael Parag and Benjamin K. Sovacool. 2016. Electricity market design for the prosumer era. *Nature Energy* 1, 4 (21 Mar 2016), 16032. https://doi.org/10.1038/nenergy.2016.32

[39] M. Quashie, F. Bouffard, C. Marnay, R. Jassim, and G. Joós. 2018. On bilevel planning of advanced microgrids. *International Journal of Electrical Power & Energy Systems* 96 (2018), 422–431. https://doi.org/10.1016/j.ijepes.2017.10.019

[40] Yu Ru, Jan Kleissl, and Sonia Martinez. 2013. Storage Size Determination for Grid-Connected Photovoltaic Systems. *IEEE Transactions on Sustainable Energy* 4, 1 (2013), 68–81. https://doi.org/10.1109/TSTE.2012.2199339

[41] Fred C Schweppe, Michael C Caramanis, Richard D Tabors, and Roger E Bohn. 2013. *Spot pricing of electricity*. Springer Science & Business Media.

[42] Tom Terlouw, Tarek AlSkaif, Christian Bauer, and Wilfried van Sark. 2019. Multi-objective optimization of energy arbitrage in community energy storage systems using different battery technologies. *Applied Energy* 239 (2019), 356–372. https://doi.org/10.1016/j.apenergy.2019.01.227

[43] Tesla. 2021. *Tesla Powerwall*. https://www.tesla.com/en_au/powerwall

[44] U.S. Energy Information Adminstration. 2017. *Annual Energy Outlook 2017 with projections to 2050*. Technical Report. www.eia.gov/aeo

[45] Hao Wang and Jianwei Huang. 2018. Incentivizing Energy Trading for Interconnected Microgrids. *IEEE Transactions on Smart Grid* 9, 4 (2018), 2647–2657. https://doi.org/10.1109/TSG.2016.2614988

[46] Lucien Werner, Adam Wierman, and Steven H. Low. 2021. Pricing Flexibility of Shiftable Demand in Electricity Markets. In *Proceedings of the Twelfth ACM International Conference on Future Energy Systems* (Virtual Event, Italy) *(e-Energy '21)*. Association for Computing Machinery, New York, NY, USA, 1–14. https://doi.org/10.1145/3447555.3464847

[47] Xu Xu, Jiayong Li, Yan Xu, Zhao Xu, and Chun Sing Lai. 2020. A Two-Stage Game-Theoretic Method for Residential PV Panels Planning Considering Energy Sharing Mechanism. *IEEE Transactions on Power Systems* 35, 5 (2020), 3562–3573. https://doi.org/10.1109/TPWRS.2020.2985765

[48] Qin Zhang and Juan Li. 2012. Demand response in electricity markets: A review. In *2012 9th International Conference on the European Energy Market*. 1–8. https://doi.org/10.1109/EEM.2012.6254817

A PROOF OF PROSUMERS' UTILITY CONCAVITY

The prosumers utility function in (2a) and (2b) can be expanded as:

$$U^{\text{pro}} = \sum_{t\in\mathcal{T}}\sum_{n\in\mathcal{N}}\Bigg[-\frac{\lambda_{n,t}\beta_n}{2\hat{x}_{n,t}}x_{n,t}^2 + \Big(\lambda_{n,t}\beta_n - p_{n,t} + \lambda_{n,t}\Big)x_{n,t} + p_{n,t}G_{n,t} - \frac{\lambda_{n,t}\beta_n\hat{x}_{n,t}}{2}\Bigg] = \sum_{t\in\mathcal{T}}\sum_{n\in\mathcal{N}} f(x_{n,t}). \tag{11}$$

Considering the fact that $f(x_{n,t})$ is a continuous quadratic function, its second derivative is given by:

$$f''(x_{n,t}) = -\frac{\lambda_{n,t}\beta_n}{\hat{x}_{n,t}} \quad \forall n\in\mathcal{N},\ \forall t\in\mathcal{T}. \tag{12}$$

Since $\lambda_{n,t} > 0$, $\hat{x}_{n,t} > 0$ and $0 < \beta_n < 1$, we then have $f''(x_{n,t}) < 0$. Thus, U^{pro} is strictly concave with respect to $x_{n,t}$.

B PIECEWISE LINEAR APPROXIMATION OF A CONCAVE FUNCTION

The linearization approximation of a concave function $f(x)$ into different regions $||\text{PW}||$ over the range $[x^{\min}, x^{\max}]$ can be written as in (13a)-(13c), while (13d)-(13e) are used to define the associated constants.

$$f(x) = f(x^{\min}) + \sum_{pw\in\text{PW}} M^{pw}u^{pw} \tag{13a}$$

$$x = x^{\min} + \sum_{pw\in\text{PW}} u^{pw} \tag{13b}$$

$$0 \le u^{pw} \le A^{pw} \quad \forall pw\in\text{PW} \tag{13c}$$

$$\sum_{pw\in\text{PW}} A^{pw} = x^{\max} - x^{\min} \tag{13d}$$

$$M^{pw} = \frac{f(\sum_{q=1}^{pw} A^q) - f(\sum_{q=1}^{pw-1} A^q)}{A^{pw}} \quad \forall pw\in\text{PW}. \tag{13e}$$

C KKT OPTIMALITY CONDITIONS

The Lagrangian function for the lower level problem in (5a)–(5d) is:

$$\mathcal{L} = -\sum_{t\in\mathcal{T}}\sum_{n\in\mathcal{N}}\Bigg[B(x_{n,t}^{\min}) + \sum_{pw\in\text{PW}} M_{n,t}^{pw}x_{n,t}^{pw} + p_{n,t}(G_{n,t} - x_{n,t}) + \sum_{pw\in\text{PW}}\mu_{n,t}^{pw,1}x_{n,t}^{pw} - \sum_{pw\in\text{PW}}\mu_{n,t}^{pw,2}\Big(x_{n,t}^{pw} - \frac{x_{n,t}^{\max} - x_{n,t}^{\min}}{||\text{PW}||}\Big) - \gamma_{n,t}\Big(x_{n,t} - x_{n,t}^{\min} - \sum_{pw\in\text{PW}} x_{n,t}^{pw}\Big) - \varphi_n\Big(x_{n,t} - \hat{x}_{n,t}\Big)\Bigg]. \tag{14}$$

Then, the KKT optimality conditions can be written as:

$$\frac{\partial\mathcal{L}}{\partial x_{n,t}} = p_{n,t} + \gamma_{n,t} + \varphi_n = 0 \quad \forall n\in\mathcal{N},\ \forall t\in\mathcal{T} \tag{15a}$$

$$\frac{\partial \mathcal{L}}{\partial x_{n,t}^{pw}} = M_{n,t}^{pw} + \gamma_{n,t} + \mu_{n,t}^{pw,1} - \mu_{n,t}^{pw,2} = 0 \quad \forall pw \in \mathrm{PW},\ \forall \mathrm{n} \in \mathcal{N},\ \forall \mathrm{t} \in \mathcal{T} \tag{15b}$$

$$\frac{\partial \mathcal{L}}{\partial \gamma_{n,t}} = x_{n,t} - x_{n,t}^{\min} - \sum_{pw \in \mathrm{PW}} x_{n,t}^{pw} = 0 \quad \forall n \in \mathcal{N},\ \forall t \in \mathcal{T} \tag{15c}$$

$$\frac{\partial \mathcal{L}}{\partial \varphi_{n}} = \sum_{t \in \mathcal{T}} x_{n,t} - \sum_{t \in \mathcal{T}} \hat{x}_{n,t} = 0 \quad \forall n \in \mathcal{N} \tag{15d}$$

$$x_{n,t}^{pw} \geq 0 \perp \mu_{n,t}^{pw,1} \geq 0 \quad \forall pw \in \mathrm{PW},\ \forall \mathrm{n} \in \mathcal{N},\ \forall \mathrm{t} \in \mathcal{T} \tag{15e}$$

$$\frac{x_{n,t}^{\max} - x_{n,t}^{\min}}{||\mathrm{PW}||} - x_{n,t}^{pw} \geq 0 \perp \mu_{n,t}^{pw,2} \geq 0 \quad \forall pw \in \mathrm{PW},\ \forall n \in \mathcal{N},\ \forall t \in \mathcal{T}. \tag{15f}$$

The complementarity constraint with the form of $a \perp b$ for $a, b \geq 0$ can be linearized by using Big M formulation provided as follows:

$$0 \leq a \leq b \cdot M \tag{16a}$$

$$0 \leq b \leq (1 - b) \cdot M \tag{16b}$$

$$b \in \{0, 1\} \tag{16c}$$

where M is a sufficiently large constant and b is the binary variable. Thus, the two constraints in (15e) and (15f) can be written as:

$$0 \leq x_{n,t}^{pw} \leq \Phi_{n,t}^{pw,1} \cdot M \quad \forall pw \in \mathrm{PW},\ \forall \mathrm{n} \in \mathcal{N},\ \forall \mathrm{t} \in \mathcal{T} \tag{17a}$$

$$0 \leq \mu_{n,t}^{pw,1} \leq (1 - \Phi_{n,t}^{pw,1}) \cdot M \quad \forall pw \in \mathrm{PW},\ \forall \mathrm{n} \in \mathcal{N},\ \forall \mathrm{t} \in \mathcal{T} \tag{17b}$$

$$0 \leq \frac{x_{n,t}^{\max} - x_{n,t}^{\min}}{||\mathrm{PW}||} - x_{n,t}^{pw} \leq \Phi_{n,t}^{pw,2} \cdot M \quad \forall pw \in \mathrm{PW},\ \forall \mathrm{n} \in \mathcal{N},\ \forall \mathrm{t} \in \mathcal{T} \tag{17c}$$

$$0 \leq \mu_{n,t}^{pw,2} \leq (1 - \Phi_{n,t}^{pw,2}) \cdot M \quad \forall pw \in \mathrm{PW},\ \forall \mathrm{n} \in \mathcal{N},\ \forall \mathrm{t} \in \mathcal{T} \tag{17d}$$

$$\Phi_{n,t}^{pw,1}, \Phi_{n,t}^{pw,2} \in \{0, 1\} \quad \forall pw \in \mathrm{PW},\ \forall \mathrm{n} \in \mathcal{N},\ \forall \mathrm{t} \in \mathcal{T}. \tag{17e}$$